

Mechanism of Electron Emission Produced by a Giant-Pulse Laser

J. F. READY

Honeywell Research Center, Hopkins, Minnesota

(Received 3 August 1964)

A spinning-prism Q -switched ruby laser, with a peak power output of 2 MW, has been employed to produce single pulses of electron emission about 100 nanoseconds long. Pulses of the order of hundreds of mA/cm² were emitted from well-cleaned tungsten, thoriated tungsten, and platinum targets in a hydrogen atmosphere at 3×10^{-8} Torr. The mechanisms for production of the electrons were investigated. No component attributable to multiphoton or other nonlinear processes was identified. The amplitudes and shapes of the electron pulses agree with calculated values based on the assumption that all the electron emission is produced by conventional thermal effects.

INTRODUCTION

PREVIOUS measurements¹ showed that metallic surfaces struck by high-power laser beams emit electrons. The laser used in these and in other similar investigations² was an ordinary laser emitting pulses of about one millisecond duration with an energy of about 0.7 J. The output of the laser consisted of a sequence of relaxation oscillation spikes of irregular amplitudes and with durations of the order of one microsecond. The electron emission occurred in spikes synchronous with the laser spikes when the radiation was focused to a small area ($\sim 10^{-3}$ cm²). Because of the sharpness of the spikes, one might infer that some nonlinear effect (e.g., two-photon photoelectric effect) was producing the electron emission. However, results¹ using different photon energies and surfaces of different work functions established that nonlinear effects were not involved in producing this emission and theoretical calculations³ showed that with the large power densities present in the laser beam, the surface temperature of the metal could rise and fall rapidly enough to explain the emission as thermionic emission from the heated surface.

The present experiment was undertaken to study the mechanisms of electron emission in more detail. We used a Q -switched laser which emitted sharp single spikes of high power radiation. This permitted analysis of the data without the complication of many relaxation oscillation spikes, and under conditions of higher power density at the target which should be more favorable for observation of possible nonlinear effects.

EXPERIMENTAL TECHNIQUES

The experimental arrangement is shown in Fig. 1. The target is a metal plate about 1 cm² in area and the

¹ D. Lichtman and J. F. Ready, *Phys. Rev. Letters* **10**, 342 (1963).

² J. J. Muray, *Bull. Am. Phys. Soc.* **8**, 77 (1963); R. E. Honig and J. R. Woolston, *Appl. Phys. Letters* **2**, 138 (1963); C. M. Verber and A. H. Adelman, *Appl. Phys. Letters* **2**, 220 (1963); R. E. Honig, *Appl. Phys. Letters* **3**, 8 (1963); F. Giori, L. A. MacKenzie, and E. J. McKinney, *Appl. Phys. Letters* **3**, 25 (1963); A. J. Alcock *et al.*, *J. Electron. Control* **16**, 75 (1964); J. K. Cobb and J. J. Muray, *Bull. Am. Phys. Soc.* **9**, 536 (1964).

³ J. F. Ready, *Proceedings of the 1964 National Electronics Conference* (to be published).

collector is a tungsten spiral through the center of which the laser beam passes. Care was taken to ensure that the beam did not strike the collector. Targets of tungsten, thoriated tungsten, and platinum were used. The electrons are drawn to the collector by an applied field of 1000 V from a dc power supply, stiffened with a 1000-pF mica capacitor to avoid clipping the current pulses. The output voltage was measured across a 100- Ω load resistor and fed through a matched impedance coaxial cable terminated in a matched load. Under these circumstances, spurious signals due to reflections from the ends of the cables are minimized and the contribution of the cable capacitance to the time constant of the equipment is eliminated. Variation of the various resistances and capacitances showed the response was not limited by the RC time constant. With this apparatus current densities of 0.1 mA/cm² could be detected.

A fraction of the laser output is picked off by reflection from a glass plate and used to trigger the detection system and to monitor the laser output pulse. The 519 oscilloscope was triggered by the output from a phototube viewing a portion of the laser output. The 543 oscilloscope was then triggered by a pulse from the delayed gate of the 519 oscilloscope. Thus the laser pulse initiated the entire recording system, allowing the synchronization of the electron emission and laser monitor traces. Synchronization was obtained by delivering a pulse from a nanosecond pulse generator to both oscilloscopes using the same cables and triggering arrangement as used for the actual data recording. In this way the relative displacements of the two scope

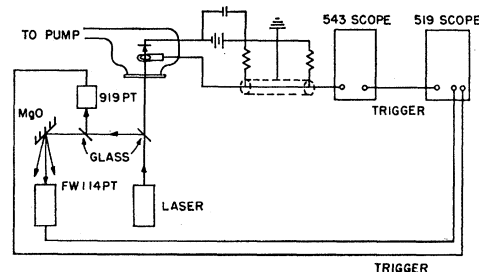


FIG. 1. Schematic diagram of apparatus.

traces caused by cable transit times and by the particular triggering arrangement could be determined and the actual relative times of the two signals could be found. Transit times of the light beam and the electrons (about one nanosecond) were included in the synchronization.

In order to have a clean reproducible surface on the target, the target was heated by rf to about 1500°K at a pressure of 2×10^{-9} Torr and then backfilled with hydrogen to a pressure of 3×10^{-8} Torr. The thoriated tungsten was activated by standard techniques.

The laser utilizes a $\frac{1}{4} \times 3$ -in. ground surface Meller ruby rod, pumped by two close-coupled *U*-shaped flashtubes. The fixed mirror is a multilayer dielectric with 65% reflectance at 6943 Å. The *Q*-switch is a Porro prism rotating at 18 000 rpm. Synchronization is provided by a magnetic pickup in the rotor, which provides a pulse to fire the power supply about 200 μ sec before the prism swings into the high *Q* position. The output pulse is a single spike 50 nsec wide at half-height with a peak power of approximately 2 MW, as measured with a calibrated S-20 phototube viewing the diffuse reflectance from an MgO block.⁴

In order to change the power density at the target, a 20-cm focal length lens could be inserted between the pickoff and the vacuum system. Data were taken both with and without the lens.

A sequence of measurements consisted of a calibration of laser power output as a function of monitor phototube pulse height, a determination of area of the spot size of the laser radiation as a function of laser power output, and a measurement of electron emission pulses for various laser power densities. To measure the area of the spot of laser radiation reaching the target, the laser was fired through 4 neutral density filters into a film plate at the same position as the target. This yielded a sharp overexposure image of the central spot with surrounding scattered light eliminated. The area of the spot was measured using a microscope. The monitor pulse height was recorded for each shot. In this way a calibration of power density in the laser beam against monitor pulse height was obtained.

Because recent theoretical work⁵ predicts a dependence of two-photon photoelectric current on the direction of polarization of the beam, the data using the thoriated tungsten target, which is of special interest because of its relatively low work function, were taken at angles of 90° and 52° between direction of polarization of the incident light and the normal to the surface.

RESULTS

The effect of collector voltage *V* was measured. For a laser pulse of constant power density, the peak electron emission increased approximately as $V^{3/2}$ at low collector voltages, and then saturated and remained constant for $V > \sim 150$ V. This was interpreted to be due to space-charge effects which were overcome at high voltages.

⁴ R. C. C. Leite and S. P. S. Porto, Proc. IEEE 51, 606 (1963).

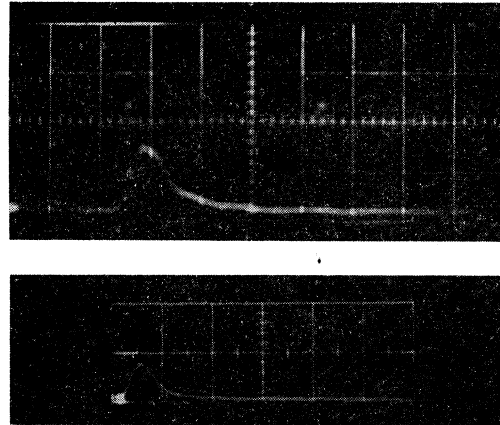


FIG. 2. Typical electron emission pulse. Upper trace is electron emission from tungsten target, 0.2 V/div, 50 nsec/div. Lower trace is the output of a monitor phototube viewing the laser output, 9.6 V/div, 50 nsec/div. The start of the lower trace is delayed by 80 nsec relative to the start of the upper trace.

The data used in later results were all taken with $V = 1000$ V.

The raw data consisted of pairs of photographic traces of the electron emission and phototube monitor outputs. A typical example of the emission from a tungsten target is shown in Fig. 2.

The electron emission began about 30 nsec after the start of the laser pulse, reached its peak value in about 30 nsec, and then fell off to the base line in about 100 nsec. From a knowledge of the spot area the current density from the area struck by the laser could be calculated. Current densities of about 50–100 mA/cm² were common and current densities as high as 480 mA/cm² were observed from tungsten. Laser power densities of about 10–25 MW/cm² were used. Below 10 MW/cm² there was no measurable electron emission. The upper limit was low enough to avoid destruction of the surface. All data were taken at power density levels where no visible damage to the surface occurred.

Analyses of these data indicate that all observed emission is thermal in origin, produced by heating of the surface and described by the Richardson equation.

This conclusion is reached because there is no observable emission at the time of peak laser power, in contradiction to what would occur if nonlinear effects were being observed. The shapes and amplitudes of the emission current pulses are approximately the same as what is calculated assuming thermionic emission produced by the given laser pulse. The delay between the start of the laser pulse and the start of the observed electron emission also is about what would be expected on a thermal basis.

Emission caused by nonlinear effects should begin earlier, peak at the same time as the laser pulse, and fall to zero at the end of the pulse. At the time when peak emission from two-photon effect should be present, the emission has not yet begun, so that the thermionic emission is not masking the other effect.

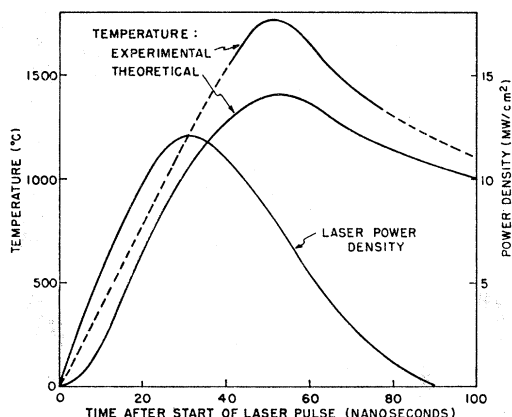


FIG. 3. Surface temperature of thoriated tungsten as function of time, determined experimentally from electron emission data and also calculated using the indicated laser pulse shape.

Figure 3 shows the laser power density as a function of time and the time dependence of the surface temperature of the thoriated tungsten target determined from the experimental electron emission data using the Richardson equation under the assumption that all emission is thermionic. It also gives the time dependence of the surface temperature as calculated theoretically by solving the differential equation for linear heat flow using the given laser pulse shape.³ There is good agreement between the shapes of the theoretical and experimental curves. The amplitudes also agree reasonably well. The difference in absolute value can be accounted for by nonuniformity of the power density in the laser beam; this will be considered later.

Figure 4 shows the peak temperature rise of the tungsten surface, again calculated from the experimental data using the Richardson equation. It also gives the theoretical curve calculated using the pulse

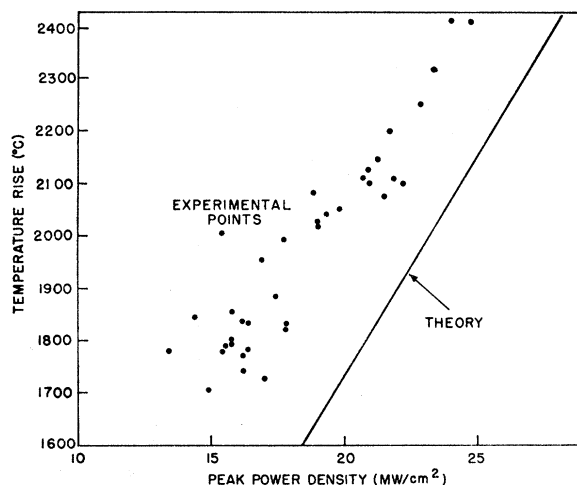


FIG. 4. Peak surface temperature of tungsten target as a function of peak laser power density, determined experimentally from electron emission data and also calculated using a laser pulse shape similar to that shown in Fig. 3.

shape shown in Fig. 3. The differences between absolute values of experimentally determined and theoretically calculated values again may be explained by nonuniformity of power density in the laser beam.

The results obtained using thoriated tungsten, tungsten, and platinum are qualitatively the same and lead to the same conclusion. The emission from thoriated tungsten did not change as the angle between the direction of polarization and the surface normal was changed.

DISCUSSION

The power density in the laser beam is not completely uniform. This nonuniformity should give a temperature value derived from observed electron emission higher than the value calculated assuming a uniform power distribution. A local hot spot in the laser beam can cause a large contribution to the emission because of the exponential dependence of emission on temperature, thus making average temperature look higher than it is. Calculations using various sample temperature distributions indicate that this effect can make the temperature appear to be several hundred degrees higher than the real average temperature. For example, let us assume a Gaussian distribution of power density within a circular spot of radius R ,

$$T(r) = T_0 e^{-r^2/R^2}.$$

We make this choice for illustrative purposes, and do not imply that this is the actual distribution. Then the true average temperature is $T_0(1 - 1/e)$, and the average emission per unit area is:

$$\begin{aligned} & \frac{1}{\pi R^2} \int_0^R AT^2(r) \exp[-\varphi/kT(r)] 2\pi r dr \\ &= AT_0^2 \left\{ \left(\frac{\varphi}{2keT_0} - \frac{1}{2e^2} \right) \exp[-\varphi e/kT_0] \right. \\ & \quad + \left(\frac{1}{2} - \varphi/2kT_0 \right) \exp[-\varphi/kT_0] \\ & \quad \left. + \frac{\varphi^2}{2k^2T_0^2} [\text{Ei}(-\varphi e/kT_0) - \text{Ei}(-\varphi/kT_0)] \right\}, \end{aligned}$$

where φ is the work function of the surface, A is the constant factor in Richardson's equation, and $\text{Ei}(x)$ is the exponential integral function. For tungsten with $T_0 = 2625^\circ\text{K}$, the average emission per unit area will be 6.65 A/cm^2 , yielding an apparent average temperature of 2140°K , whereas the true average temperature is 1660°K . This difference is roughly the same as the differences between theoretical and experimental values shown in Figs. 3 and 4.

Several theoretical estimates of the two-photon photoelectric current expected to be produced by a laser beam have appeared.⁵⁻⁷ Using Eqs. (3.11) and

⁵ I. Adawi, Phys. Rev. **134**, A788 (1964).

⁶ R. L. Smith, Phys. Rev. **128**, 2225 (1962).

⁷ P. Bloch, J. Appl. Phys. **35**, 2053 (1964).

(3.14) of Ref. 5, we calculate a peak photocurrent of 25 mA/cm² from the thoriated tungsten surface when a ruby laser beam of power density 20 MW/cm² is incident on the surface at an angle of 52° between the direction of polarization and the surface normal. This current density should have been easily detectable with this apparatus and should have occurred at a time when it would not be masked by thermionic emission. There was no trace of electron emission from thoriated tungsten with the right time dependence for two photon effect. If such emission was present, it must have been considerably smaller.

In the calculations of temperature rise given in Figs. 3 and 4, reflectivity of the surface has been neglected; it was assumed that all energy in the laser beam was absorbed. The inclusion of reflection of energy from the

surfaces would tend to increase the differences between the experimental and theoretical curves in Figs. 3 and 4. The results indicate that a considerable portion of the energy was absorbed, even though the surfaces appeared initially shiny. As the surface begins to heat early in the high power density pulse, the absorption may increase rapidly. Other results³ on the depth of holes vaporized in metallic surfaces also indicate that a large fraction of the energy in the laser pulse is absorbed.

ACKNOWLEDGMENTS

The author wishes to thank A. W. Ryberg, V. Snerberg, and K. R. Engh for their assistance in performing the measurements, and E. Bernal and D. Lichtman who contributed valuable discussions and constructive criticism.

Injection Luminescence in GaAs by Direct Hole-Electron Recombination

J. C. SARACE, R. H. KAISER, J. M. WHELAN, AND R. C. C. LEITE*

Bell Telephone Laboratories, Murray Hill, New Jersey

(Received 27 August 1964)

Luminescence from GaAs *p-n* junctions was measured under conditions where spectral distortion due to self-absorption was $\leq 15\%$. Spectra were observed through a 2-3- μ -thick Zn-diffused *p*-type layer ($C_0 \approx 5 \times 10^{19}$ cm⁻³) and a thin Au contact. Junctions in a float-zone-refined crystal, $n = 2 \times 10^{16}$ cm⁻³, showed a dominant emission band with peak energies of 1.423 and 1.508 eV when measured in ambients of 298 and 77°K, respectively. This band is attributed to direct hole-electron recombination resulting from hole diffusion into the *n*-type region of these *p-n* junctions. Supportive evidence includes good correspondence with the calculated emission peak based on detailed balancing arguments and optical absorption data, independence of peak energy on junction voltages at low current densities, and agreement with photoluminescent data for *n*-type GaAs. The recombination process responsible for this band is significant for diodes with $n = 2.3 \times 10^{17}$ cm⁻³ at room temperature, but not at 77°K, nor for diodes with $n = 2 \times 10^{18}$ cm⁻³ at either temperature.

SPONTANEOUS injection luminescence of forward biased GaAs *p-n* junctions has been measured with special emphasis on the reduction of spectral distortion. Principal sources of distortion are self-absorption and internal reflection within the GaAs. A new emission band has been observed from junctions made by Zn diffusion into lightly doped *n*-type samples where $n = 0.2$ to 2×10^{16} cm⁻³. The above emission band at 298 and 77°K matches the one calculated from Sturge's absorption data,¹ the principle of detailed balance, and the assumption of a negligible contribution by phonon-assisted transitions. This agreement supports Sturge's energy assignment of the direct energy gap of GaAs at these temperatures. We attribute this band to direct hole-electron recombination on the *n*-type side of the junction under conditions where the conduction band minimum and valence band maximum are essentially

unperturbed by low concentrations of impurities. In the context of this report, direct recombination includes radiative recombination via free exciton annihilation and direct band-to-band transitions, i.e., those responsible for absorption at the edge.

The diode structure shown in Fig. 1 was used to reduce spectral distortion of luminescence originating in the vicinity of the junction. The 120- μ -thick *p*-type layer on the back side was made by Zn diffusion for 5 h at 750°C from a ZnO-GaAs powder source in a sealed ampule.² This serves as an absorber for that radiation not absorbed in the *n*-type region and acts as the equivalent of an antireflective coating. The active junction 2-3 μ below the top mesa surface was made subsequently by a similar diffusion for 2 h at 650°C. Surface concentrations of the shallow and deep diffused layers are estimated to be 5×10^{19} and 2×10^{20} cm⁻³, respectively. The shallow *p* layer was contacted by reaction

* On leave of absence from the Instituto Tecnológico de Aeronáutica, Brazil.

¹ M. D. Sturge, Phys. Rev. **127**, 768 (1962).

² L. A. D'Asaro (private communication).

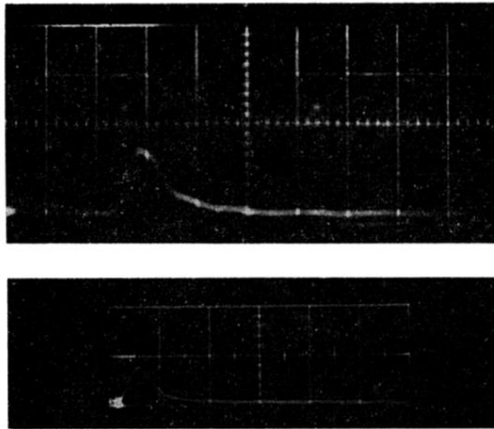


FIG. 2. Typical electron emission pulse. Upper trace is electron emission from tungsten target, 0.2 V/div, 50 nsec/div. Lower trace is the output of a monitor phototube viewing the laser output, 9.6 V/div, 50 nsec/div. The start of the lower trace is delayed by 80 nsec relative to the start of the upper trace.